

Article - Human and Animal Health

FAM224A/hsa-mir-139/RAD54B is a Competing Endogenous RNA Network that may Serve as a New Prognostic Factor and Treatment Target for Liver Cancer

Wei Jiang¹

<https://orcid.org/0000-0003-4239-1831>

Wei Lu²

<https://orcid.org/0000-0003-4920-0276>

Wenjie Yang^{1*}

<https://orcid.org/0000-0002-9608-2770>

¹Tianjin First Central Hospital, Department of Infectious Diseases, Tianjin, China. ²Tianjin Medical University Cancer Institute & Hospital, Liver cancer center, Tianjin, China.

Editor-in-Chief: Paulo Vitor Farago
Associate Editor: Marcelo Ricardo Vicari

Received: 01-Nov-2021; Accepted: 28-Apr-2022.

*Correspondence: nankaidoc@nankai.edu.cn; Tel.: +86-022-23626776 (W.L.)

HIGHLIGHTS

- A HCC-associated competing endogenous RNAs network, FAM224A/hsa-mir-139/RAD54B, was established in this study.
- FAM224A/hsa-mir-139/RAD54B played an important role on HCC progression and metastasis.
- We revealed that FAM224A may be an important prognostic factor and treatment target for HCC.

Abstract: The potential of long noncoding RNAs (lncRNAs) as symptomatic and prognostic biomarkers in oncotherapy for hepatic carcinoma has been revealed. However, the specific mechanisms of lncRNA-regulated tumor progression and metastasis are not completely known. The RNA and miRNA sequencing data of liver cancer in The Cancer Genome Atlas database were analyzed. A competing endogenous RNA (ceRNA) was constructed, and its effects on the progression and metastasis of tumors and the survival rates of patients with tumor were evaluated. Differentially expressed mRNAs, miRNAs, and lncRNAs were identified. A liver cancer-associated ceRNA network, namely, FAM224A/hsa-mir-139/RAD54B, was then established. FAM224A/hsa-mir-139/RAD54B assumed a significant part in liver malignancy movement and metastasis. A series of cell experiments was conducted to prove the importance of ceRNAs, and the binding between RNAs was validated through a dual-luciferase reporter assay. The FAM224A/hsa-mir-139/RAD54B network in liver cancer was identified. FAM224A may be an important prognostic factor and treatment target for liver cancer.

Keywords: long noncoding RNAs; biomarkers; hepatic carcinoma.

INTRODUCTION

Hepatic carcinoma is one of the frequently occurring cancers in the world, which has a high morbidity and mortality [1]. It has no apparent symptoms in patients but has a strong invasion and metastasis potential. Patients are usually diagnosed at advanced stages when appropriate therapeutic options are limited and ineffective [2-4]. Therefore, novel molecular biomarkers and therapeutic targets are necessary.

Noncoding RNAs (ncRNAs), including microRNAs (miRNAs), small nucleolar RNAs (snoRNAs), ribosomal RNAs (rRNAs), transfer RNAs (tRNAs), and long noncoding RNAs (lncRNAs), have many functions in tumor progression and metastasis [5, 6] and have no ability to encode proteins. Moreover, lncRNAs and miRNAs are mainly involved in tumor progression and metastasis, so they are potential drug targets [7-9]. lncRNAs participate in cell cycle, cell differentiation, and epigenetic regulation [10-12]. They may also be used as symptomatic and prognostic biomarkers in oncotherapy for Hepatic carcinoma. However, the specific mechanisms of lncRNA-regulated tumor progression and metastasis are not completely known [13].

Salmena and coauthors were the first to introduce competing endogenous RNAs (ceRNAs) [14]. lncRNAs can act as ceRNAs to crosstalk with other RNA transcripts. Generally, miRNAs inhibit or degrade mRNAs [15, 16], and lncRNAs compete with mRNAs to target miRNAs. This ceRNA hypothesis is supported by substantial experimental evidence [17-19]. Until now, lncRNA-miRNA-mRNA networks have been analyzed in many human malignancies [20, 21]. However, liver cancer-associated ceRNA regulatory networks is poorly characterized.

In this examination, the mRNA and miRNA sequencing information of hepatic carcinoma in The Cancer Genome Atlas (TCGA) data set were used to analyze. Differentially expressed (DE) mRNAs (DEmRNAs), miRNAs (DEmiRNAs), and lncRNAs (DElncRNAs) were distinguished, and a hepatic carcinoma related ceRNA network was set up.

The family with sequence similarity 224 member A (FAM224A) combine with miR-590-3p in glioma cells to regulate the expression level of miRNA, which can inhibit the growth of tumor. However, the function of the lncRNA FAM224A in human hepatic carcinoma is not clear. In this investigation, lncRNA FAM224A was distinguished as a feasible prognostic factor and therapy target for hepatic carcinoma.

MATERIAL AND METHODS

Cell culture

The human cell line HepG2 (KeyGen Biotech, Nanjing, China) was authenticated via short tandem repeat profiling. HepG2 cells were cultured in DMEM (Hyclone, USA). Cells were cultured in 37 °C and 5% CO₂ environment.

Cell transfection

HepG2 cells were cultivated in six-well plates and developed to 4 × 10⁵ cells for each well. Small interfering RNA (siRNA) against FAM224A, the scrambled siRNA of FAM224A, the plasmid carrying the FAM224A gene, the blank control of the plasmid, the hsa-mir-139 mimic, and the negative control were transfected with Lipofectamine 3000 (Invitrogen, Carlsbad, CA, USA) as per the producer's directions. RNA was synthesized and designed with GeneCopoeia (Guangzhou, China).

Real-time polymerase chain reaction (RT-PCR)

The extraction of Total RNA was used with TRIzol reagent (Invitrogen, USA) from MCF-7 cells. cDNA was synthesized with Oligo (dT) or random primers by using a Quantscript RT kit (Tiangen, China). The mRNA expression levels of FAM224A, RAD54B, and β-actin were examined with a SYBR RT-PCR kit (Tiangen, China). A TaqMan MicroRNA reverse transcription kit and TaqMan Universal Master Mix II (Tiangen, China) were utilized to analyze the expression levels of hsa-miRNA-139 and U6. After normalizing the expression level to endogenously control β-actin or U6, the relative expression value was calculated by 2^{-ΔΔCt} method to represent the multiple changes of gene expression. The primer sequence designed by primer Premier 5.0 is shown in Table 3.

Collection of clinical data and RNA-seq data

An aggregate of 374 data of patients with hepatic carcinoma were given acquired from TCGA database (<https://cancergenome.nih.gov/>). A total of 358 patients had complete clinical information (i.e., gender, race,

stage, days, volume, grade, and status). lncRNA, miRNA, and mRNA sequence data included 50 paracancerous samples and 374 hepatic carcinoma samples got from TCGA. Perl was used to extract a transcriptome expression matrix from the RNA-sequencing data in TCGA.

Analysis of DE genes

Using the edgeR software package of Bioconductor Analysis Tool for R (a statistical method of negative binomial distribution) to distinguish differentially expressed genes. Genes that meet condition $|\logFC| > 1$, $FDR < 0.05$ are considered as DE genes.

Weighted correlation network analysis (WGCNA) was used to perform coexpression network analysis on RNA expression information of the hepatic carcinoma samples. The purpose of WGCNA was to find co-expressed gene modules, further to explore the connection between core genes in the network and the connection between the genes and phenotypes. The correlation coefficient between genes was calculated by the Pearson method. Before the R package was utilized for WGCNA, 6,356 DE mRNAs, 2,699 DE lncRNAs, and 320 DE miRNAs were integrated and normalized into a single matrix. Finally, 358 tumor tests samples extensive clinical information were filtered into the investigation. Clinical information of patients included gender, age, survival status, survival time, clinical stage, clinical grade, and race. Construct a scale-free co-expression network with a weight of β , and calculate the adjacency relationship between genes. Quantify the similarity between genes according to the contiguity, and deduce the dissimilarity coefficient between genes. A systematic clustering tree between genes was drawn accordingly. In accordance with the criteria of the mixed dynamic cut tree, we chose 30 as the minimum number of genes in each gene module [22]. The modules were determined by the dynamic shearing method, the eigenvector values of each module were measured. The modules were clustered and analyzed, and modules with close distances were integrated into a new module. Correlation between the eigenvalues of each module and clinical information was obtained, and the gene module most closely related to liver cancer was identified.

Cell proliferation assay by cell counting kit-8

Cells are cultivated in 96-well plates and the concentrations are set to 7000 cells/well. After every 24 h, we pour 10 μL of Cell Counting Kit-8 (CCK-8) solution into each well and incubate it for 2 h. Then, we measure $\text{OD}_{450 \text{ nm}}$. This process was repeated eight times for each test.

Matrigel invasion test

Cell invasion tests were conducted in a Transwell chamber (Corning, USA), and filters were coated with Matrigel (BD, USA). HepG2 cells were inoculated into Transwell upper compartment in serum-free culture, while a medium containing 10% fetal bovine serum was placed in the lower compartment to induce cell invasion. 24 h later, the cells were fixed in 4% paraformaldehyde and dyed by crystalline violet. Counting was conducted under an optical microscope (Nikon, Japan).

Clone formation test

The cells in each group in were digested, seeded into a six-well plate, incubated for 10 days, fixed with 95% methanol (4%, 15 min, and 37 °C), and stained with crystal violet for 10 min. Colony numbers with less than 50 cells were analyzed with an Olympus digital camera. Experiments were repeated at least thrice.

Wound healing test

Cells were inoculated at a concentration of 5×10^5 cells/well in 24-well culture plates. After they were incubated overnight, using the tip of a 200 μL pipette to scrape cells adhering to the bottom of the well. Cells were washed with phosphate-buffered saline and then incubated in serum-free conditions for 24 and 48 hours. Images of wounds were obtained with a light microscope (Nikon, Japan).

Dual-luciferase reporter test

After the binding site was predicted by the DIANA tool, the binding site and its mutant sequence were inserted into the psiCHECK2 dual-luciferase reporter vector (Promega, Madison, WI). They were transferred into has-miR-139 mimic HepG2 cells and their control cells through reference cell transfection method. After transfection, cultivated cells for 48 h and then lysed with lysis buffer. Luciferase Assay Reagent II was added,

and data (firefly luciferase) were measured. Add Stop&Glo reagent to measure the intensity of Renilla luciferase. Each experiment was repeated thrice.

Animal studies

BALB/c nude mice (15–18 g) were purchased from the Animal Center Academy of the Military Medical Science (Beijing, China). These mice were bred under specific pathogen-free conditions. All procedures were approved based on guidelines of the Animal Ethics Committee of Tianjin Medical University. Different kind of HepG2 cells were injected in subcutaneous tissue of the mouse (1×10^6 cell per mouse, 5 mice per group). Tumor volume was measured every day. Lastly, the mice were sacrificed in a humanitarian manner, and tumor tissues were measured.

Statistical analysis

The significance of the experimental results was evaluated through two-sided tailed Student's test in wound healing tests, dual-luciferase reporter tests, clone formation tests, tube formation test, and RT-PCR. Survival analysis was conducted by Kaplan-Meier method and significance testing was conducted by log-rank test. All error bars represented mean \pm SEM. All hypothesis tests were considered statistically significant at $P < 0.05$.

RESULTS

Identification of DElncRNAs, DEmRNA, and DEmiRNA based on the TCGA data of liver cancer

The RNA-seq sequencing data, including 374 tumor tissues and 50 paracancerous tissues, of 424 patients with liver cancer were downloaded from TCGA database. EdgeR package was used in the analysis of DE genes. A gene with $|\log_{2}FC|$ of >1 and FDR of <0.05 was considered to be DE. Finally, 6,356 DE mRNAs (3,758 upregulated mRNAs and 2,598 downregulated mRNA, Figures 1A and 1B), 2,699 DElncRNA (2,297 upregulated lncRNAs and 402 downregulated lncRNAs, Figures 1C and 1D), and 320 DEmiRNA (270 upregulated miRNAs and 50 downregulated miRNAs, Figures 1E and 1F) were obtained. In the figures, downregulated genes were shown in green, upregulated genes were presented in red, and genes without significant changes were marked black.

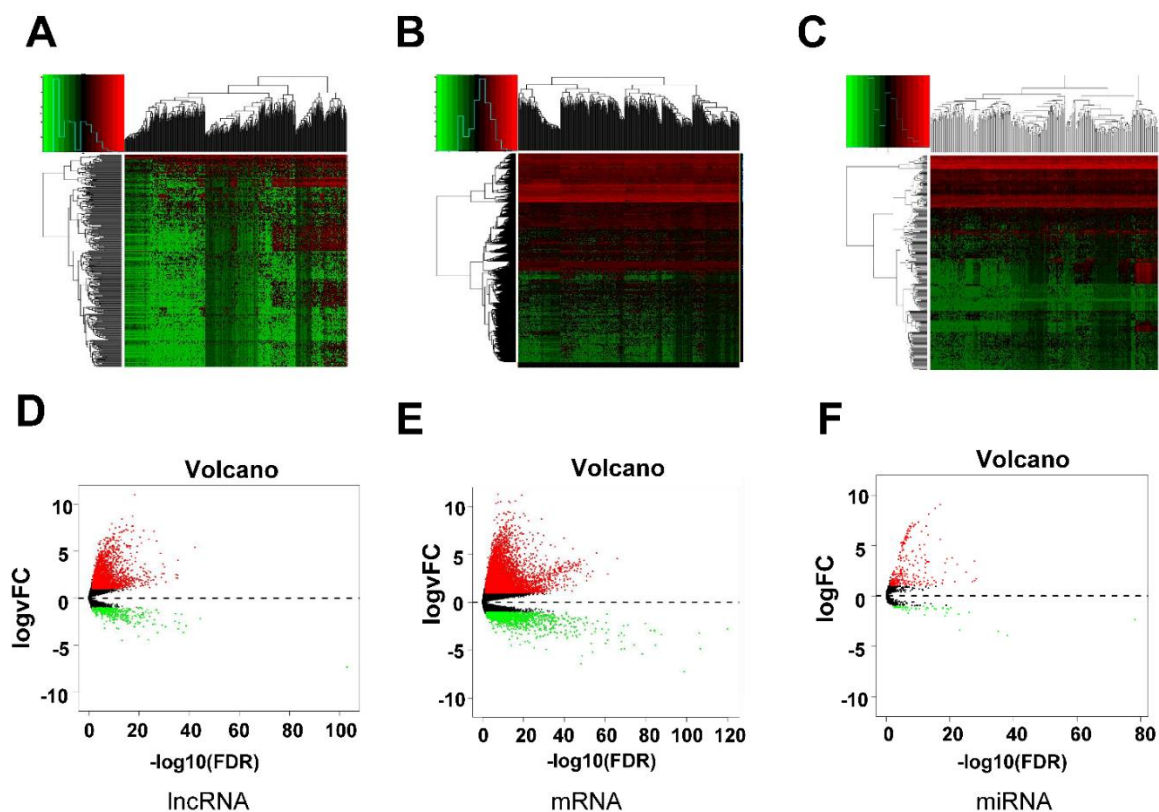


Figure 1. RNA expression heatmap and volcano map of liver cancer samples and paracancerous samples from TCGA. (A) mRNA, (B) lncRNA, and (C) miRNA.

Construction of a lncRNA–miRNA–mRNA co-expression scale-free network

A lncRNA–miRNA–mRNA co-expression network was established. WGCNA was performed to set up a co-expression network. Expression data (TMM) in DE mRNA, DE lncRNA, and DE miRNA were combined into the same matrix as input files for analysis.

Network average connectivity was calculated for different β values to select the appropriate β value (Figure 2A). A β value of 4 was considered the best choice. When $\beta = 4$, the k value of the node approximated the power law distribution (Figure 2B). The genes were divided into 12 modules, and genes inside each module had similar expression characteristics and biological functions (Figure 2C).

Clinical data from patients with liver cancer were downloaded from TCGA database, and the correlation between each module and clinical feature was calculated. The results showed that the purple module had the strongest negative correlation with pathological grade, clinical stage (Figures 2D and 2E), and patients' survival times. The network contained 48 nodes, including 2 miRNAs, 10 lncRNAs, and 46 mRNAs (Figure 2F). DE analysis showed that hsa-mir-1197 was upregulated in the tumors, whereas hsa-mir-139 was downregulated. The 10 lncRNAs were AC092171.2, AC132192.2, AC004477.1, AC239868.2, AC138356.1, AL606489.1, FAM224A, AC005332.8, and SNHG4. These lncRNAs except AC138356.1 were overexpressed in the liver cancer sample (Table 1).

Table 1. Differences in the expression levels of lncRNA and miRNA in the network between liver cancer and paracancerous samples from TCGA. $\log_{2}FC = \log_{2}(\text{cancer}) - \log_{2}(\text{control})$; FDR is the P value corrected via the Benjamini–Hochberg multiple test.

Gene	logFC	PValue	FDR	Type
AC092171.2	2.651829972	3.58E-44	8.30E-42	up
AC132192.2	2.43309798	1.59E-38	2.28E-36	up
AC004477.1	2.808776898	2.65E-37	3.31E-35	up
AC239868.2	2.181734923	1.78E-33	1.58E-31	up
AC138356.1	-2.259640873	2.20E-31	1.57E-29	down
AL606489.1	3.123917152	1.91E-31	1.38E-29	up
FAM224A	2.938576075	2.83E-07	1.01E-06	up
AC005332.8	1.652014456	3.90E-31	2.68E-29	up
SNHG4	2.439786999	4.78E-20	7.40E-20	up
hsa-mir-1197	1.368137756	0.01674537	0.047465735	up
hsa-mir-139	-1.632754924	4.62E-29	8.90E-27	down

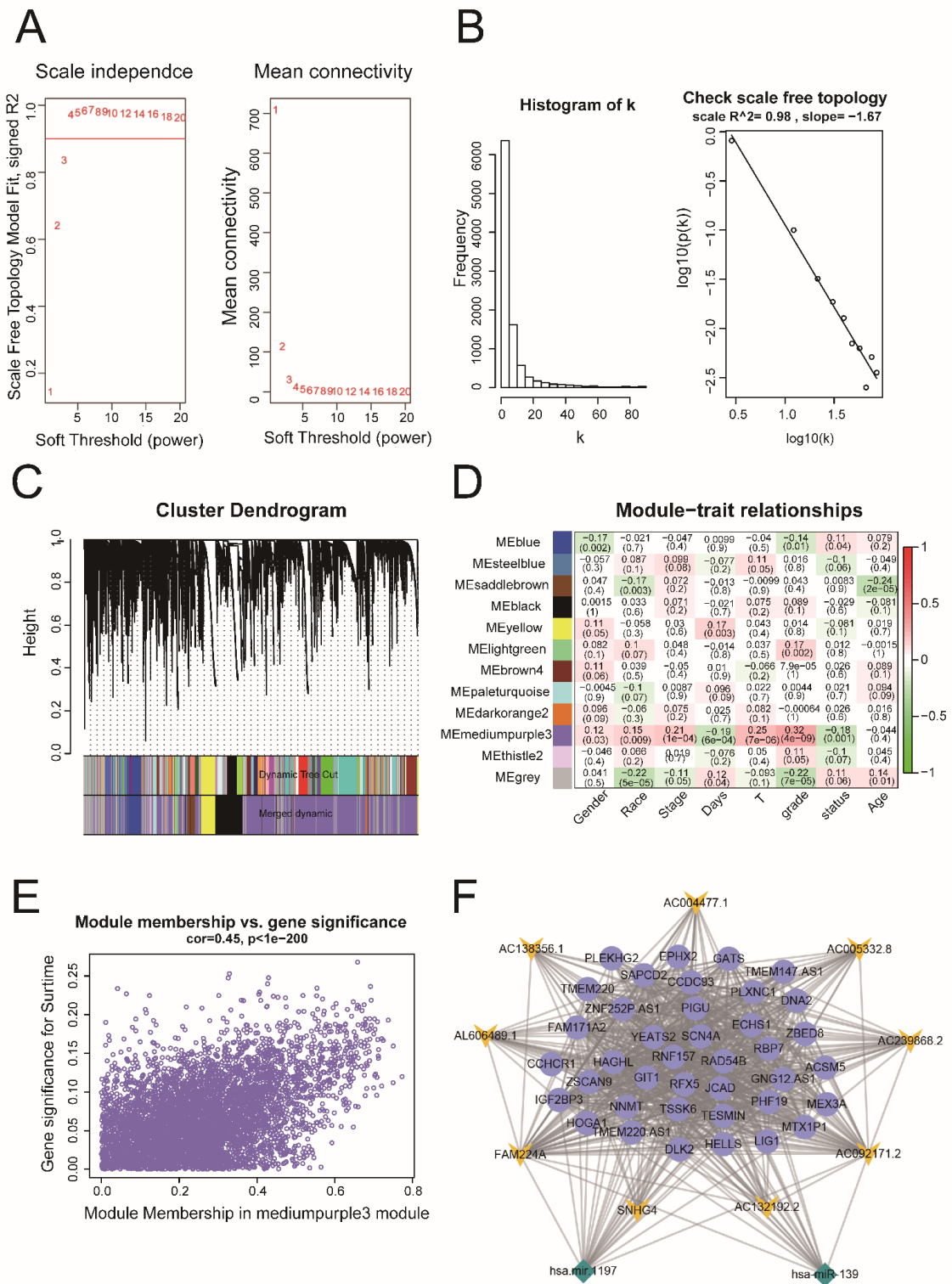


Figure 2. WGCNA and co-expression network analysis. (A) Scale independence and average connectivity corresponded to different beta values. (B) $\beta = 4$; the distribution of the degree-k value of the nodes in the network approximated the power law distribution and fitted well with the ideal natural distribution function $p(k)$ of the k value. (C) A systematic tree diagram of weighted gene co-expression network analysis was shown. Initial module partitioning is first calculated by using the dynamic rolling shear algorithm, and modules were merged on the basis of the similarity of the feature vector values of each module. Finally, 12 gene modules were obtained. (D) A heatmap of the correlation of gene modules with various clinical features was presented. The purple module had the strongest negative correlation with survival time and the strongest positive correlation with clinical stage and pathological grade. (E) The eigenvalues of genes in the purple module were strongly correlated with survival time. (F) Co-expression relationship with a weight value of ≥ 0.7 in the purple module was illustrated. Green dots represented mRNAs, red dots indicated lncRNAs, and blue dots denoted miRNAs.

Binding of hsa-mir-139 to FAM224A and RAD54B

Co-expression and sequence analysis showed that FAM224A/hsa-mir-139/RAD54B were ceRNAs. Luciferase reporter plasmids containing 3'UTR sections of FAM224A and RAD54B were constructed by using hsa-mir-139 and conducting a dual luciferase reporter assay to finalize their binding relationship and binding sequence. In addition, plasmids containing the mutant sections of FAM224A were constructed on the basis of the binding sites predicted by the DIANA tool. The results indicated that the luciferase activity of the wild-type FAM224A reporter vector was decreased due to hsa-mir-139 overexpression. However, the signal increased again when hsa-mir-139 and RAD54B were overexpressed and this effect did not occur in the wild type (Figure 3A). Similar results were found in the luciferase assay of RAD54B (Figure 3B).

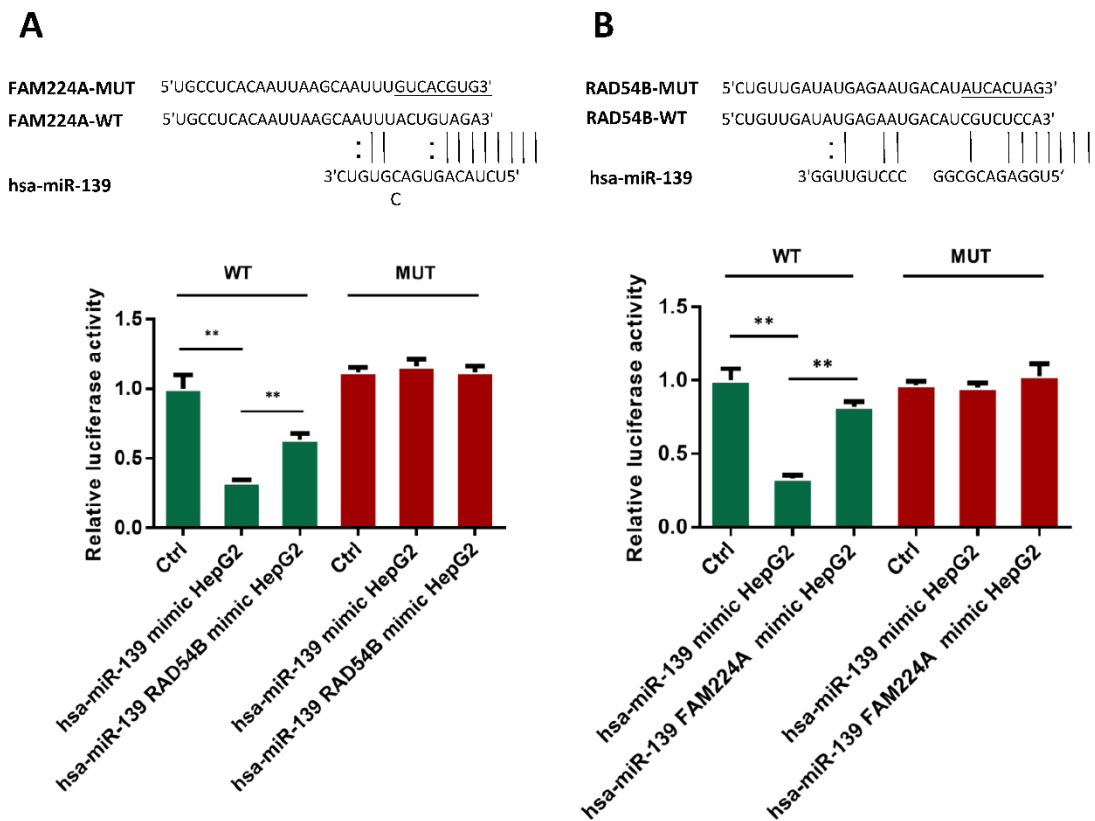


Figure 3. Direct binding of Hsa-mir-139 to FAM224A and RAD54B. (A) Dual-luciferase reporter test revealed a binding site for FAM224A and hsa-mir-139. For mutant dual-luciferase plasmids, the overexpression of hsa-mir-139 alone led to a significant decrease in the signal, whereas the overexpression of both hsa-mir-139 and FAM224A caused this effect to disappear to a certain extent. This effect did not occur in the mutant assay. (B) Similar to FAM224A, RAD54B and hsa-mir-139 had binding sites. Mean ± SD; *P < 0.05; **P < 0.01, ***P < 0.001.

Potential competing endogenous RNAs: FAM224A/hsa-mir-139/RAD54B

Only FAM224A/hsa-mir-139 was negatively correlated in the lncRNA–miRNA co-expression relationship in this co-expression network. Therefore, FAM224A/hsa-mir-139 showed potential for binding. The DIANA tool was utilized to predict the lncRNA that might bind to hsa-mir-139. The threshold of the miTG score was 0.99. In Table 2, the miTG score of FAM224A was 0.998, which was consistent with our previous conjecture. The DIANA tool was also used to find the mRNA that might bind to hsa-mir-139, and the threshold of the miTG score was set to 0.9. The results revealed that RAD54B was the only mRNA that had a co-expression relationship with hsa-mir-139, so RAD54B might bind to hsa-mir-139 (Table 2). RAD54B was upregulated in liver cancer and negatively correlated with hsa-mir-139. Therefore, FAM224A, hsa-mir-139, and RAD54B were potential ceRNAs.

Table 2. Prediction of mRNA and lncRNA that might bind to hsa-mir-139 via the DIANA tool. miRNA target gene (miTG) score is a comprehensive combination forecast index in DIANA tool obtained with the following: miTG score $\in [0,1]$. The higher the miTG score, the greater the possibility of binding.

target mRNA	miTG score	target lncRNA	miTG score
RP11-297N6.4	0.999997387	LINC00662	1
UBR4	0.994537097	chr22-38_28785274-29006793.1	1
SYT2	0.992896947	RP11-678G14.4	1
ELK1	0.979865952	XLOC_001668	1
UBE2G1	0.978283897	ANKRD62P1-PARP4P3	1
ARPC1A	0.976478901	XLOC_004143	1
FAM161A	0.975118807	NR2F1-AS1	0.999
RPS15A	0.970840751	RP11-434D2.2	0.999
ANXA2R	0.967670285	RP11-219A15.2	0.999
DNMT3A	0.966236908	XLOC_003233	0.999
GNB5	0.963469494	FAM224A	0.998
SRSF3	0.962922755	XLOC_001935	0.998
AGPAT3	0.961735116	ANKRD62P1-PARP4P3	0.998
RAD54B	0.958380461	NR2F1-AS1	0.997
TTLL6	0.956517555	AC006548.28	0.995
RAB1A	0.956047497	RP11-679B19.1	0.995
PLP1	0.953598797	CH17-264L24.1	0.992
GLYR1	0.94863118	CTC-265F19.1	0.991
RBMXL2	0.947979307		
C19orf35	0.947265339		
PDE4A	0.942681521		
ZBTB10	0.940179895		
NUTM2E	0.935623589		
RGS17	0.93526549		
SERF1A	0.934998234		
PCBP4	0.932440217		
RP13-512J5.1	0.928699663		
UVRAG	0.92499542		
COX16	0.924338203		
DPP4	0.921635255		
ERVV-1	0.912963846		

FAM224A, hsa-mir-139, and RAD54B were associated with poor prognosis

The WGCNA results suggested that the genes from purple module were associated with pathological stage, clinical grade, and patient survival. As expected, the life expectancy of patients with high FAM224A and RAD54B expression levels was below observably that of patients with low FAM224A and RAD54B expression levels. By contrast, the life expectancy of patients in the group with a high hsa-mir-139 level was observably higher than that of patients with a low hsa-mir-139 expression level (Figures 4A–4C).

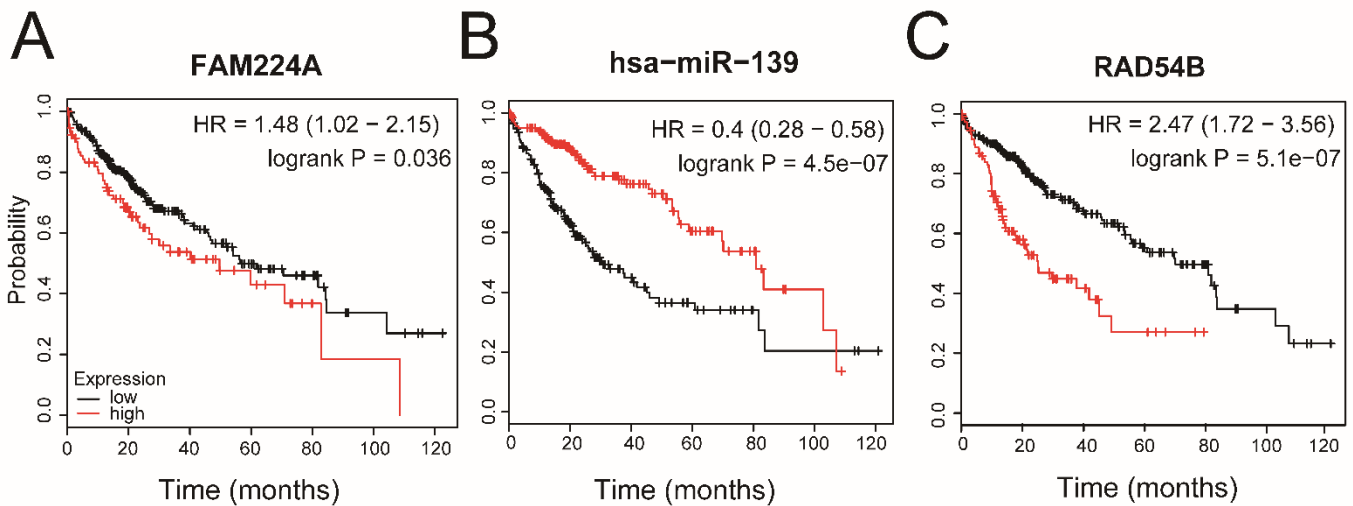


Figure 4. KM survival analysis of FAM224A, hsa-mir-139, and RAD54B in patients with liver cancer. (A) FAM224A, (B) hsa-mir-139, and (C) RAD54B. TCGA data revealed that patients with high expression levels of FAM224A and RAD54B had short survival times, whereas patients with a high expression level of hsa-mir-139 had long survival times. Mean \pm SD; *P < 0.05; **P < 0.01, ***P < 0.001.

Negative regulation of hsa-mir-139 expression and positive regulation of RAD54B by FAM224A in HepG2 cells

siRNA sequences targeting FAM224A (siFAM224A) or scrambled siRNA (sictrl) in HepG2 cells, transfected plasmids expressing FAM224A (OEFAM224A), and an empty plasmid (OEctrl) were transfected for further analysis. The effect of transfection was tested. Figure 5A shows that FAM224A was successfully overexpressed and inhibited.

The expression levels of transfected cell lines were measured by conducting qRT-PCR to initially investigate the regulatory effects of FAM224A on hsa-mir-139 and RAD54B. The results indicated that the FAM224A overexpression led to the downregulation of hsa-mir-139 and the upregulation of RAD54B (Figure 5B). Furthermore, the knockdown of FAM224A caused the upregulation of hsa-mir-139 and the downregulation of RAD54B (Figure 5C).

The expression of hsa-mir-139 was knocked down in all relevant cells based on a previous research (Figure 5D). ANOVA revealed no significant difference in the hsa-mir-139 expression levels in the four cell lines after miRNA was knocked down, and the pattern of the FAM224A expression was similar to that before the knockdown (Figure 5E). The only difference was that changes in the FAM224A expression could not affect the RAD54B expression after hsa-mir-139 knockdown. This result further confirmed our previous findings (Figure 5F).

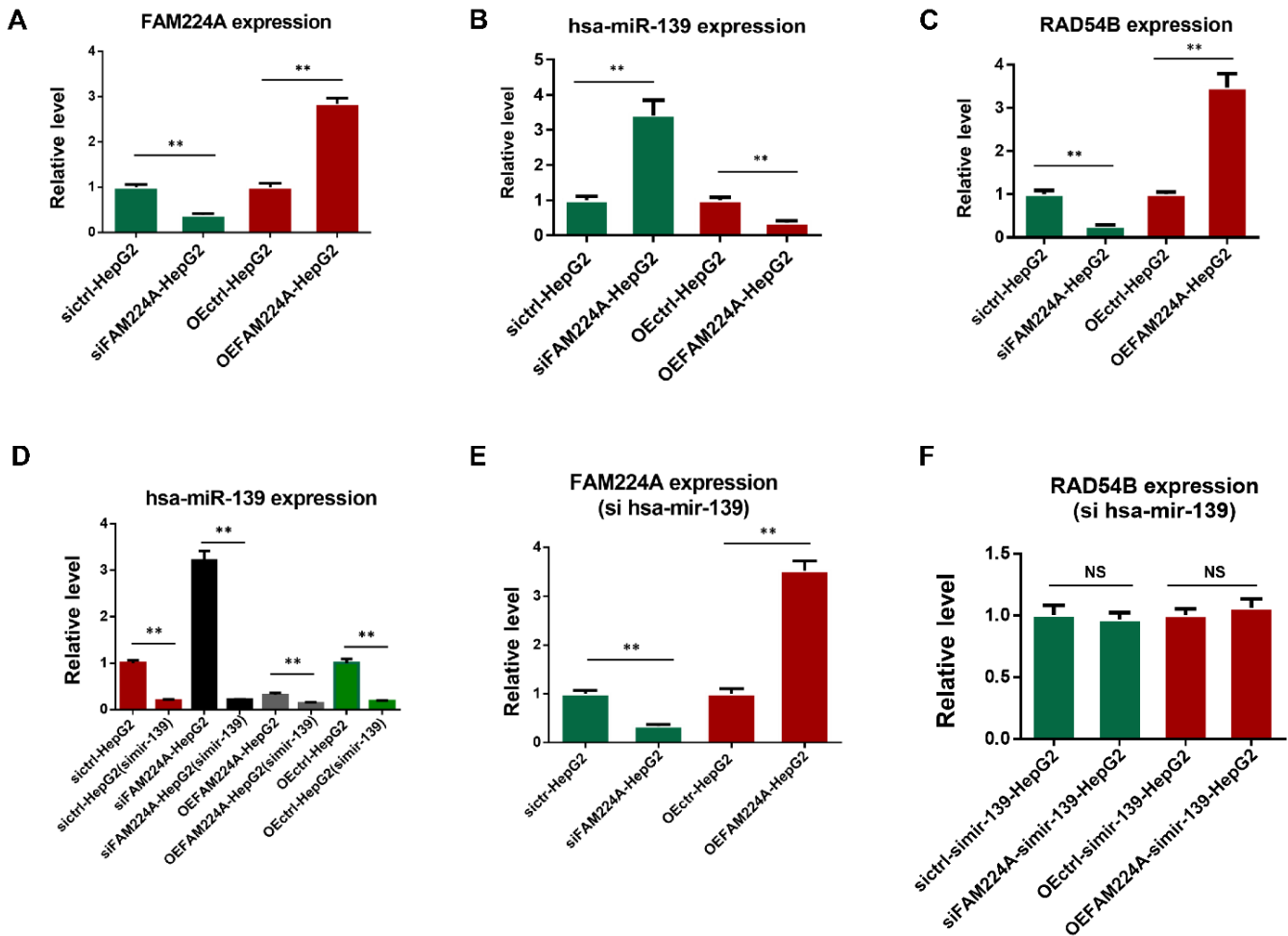


Figure 5. Effect of FAM224A on hsa-miR-139 and RAD54B expression levels. (A) FAM224A expression in HepG2 cells transfected with overexpressed plasmid and siRNA was detected through a qRT-PCR assay. FAM224A expression was successfully regulated. (B) FAM224A was upregulated after hsa-miR-139 was downregulated, and vice versa. (C) FAM224A could upregulate RAD54B expression, and vice versa. (D) hsa-miR-139 was further knocked down. The figure showed the relative expression of hsa-miR-139 before and after knockdown. (E) After hsa-miR-139 was knocked down, the control of FAM224A was still stable. (F) After hsa-miR-139 was knocked down, changes in FAM224A could no longer affect the RAD54B expression. Mean \pm SD; *P < 0.05; **P < 0.01, ***P < 0.001.

FAM224A enhanced the multiplication, migration, angiogenesis, and invasion of HepG2 cells

FAM224A may be related to the prognosis and degree of tumor malignancy. A series of experiments was performed to investigate the biological function of FAM224A in HepG2 cells and further understand the mechanisms of FAM224A on tumor cells.

The results showed that the proliferative capacity, migration ability, and invasive ability of FAM224A-overexpressing HepG2 cells were enhanced. The tumor-related functions of HepG2 cells knocked down by siFAM224A were inhibited (Figures 6A–6F).

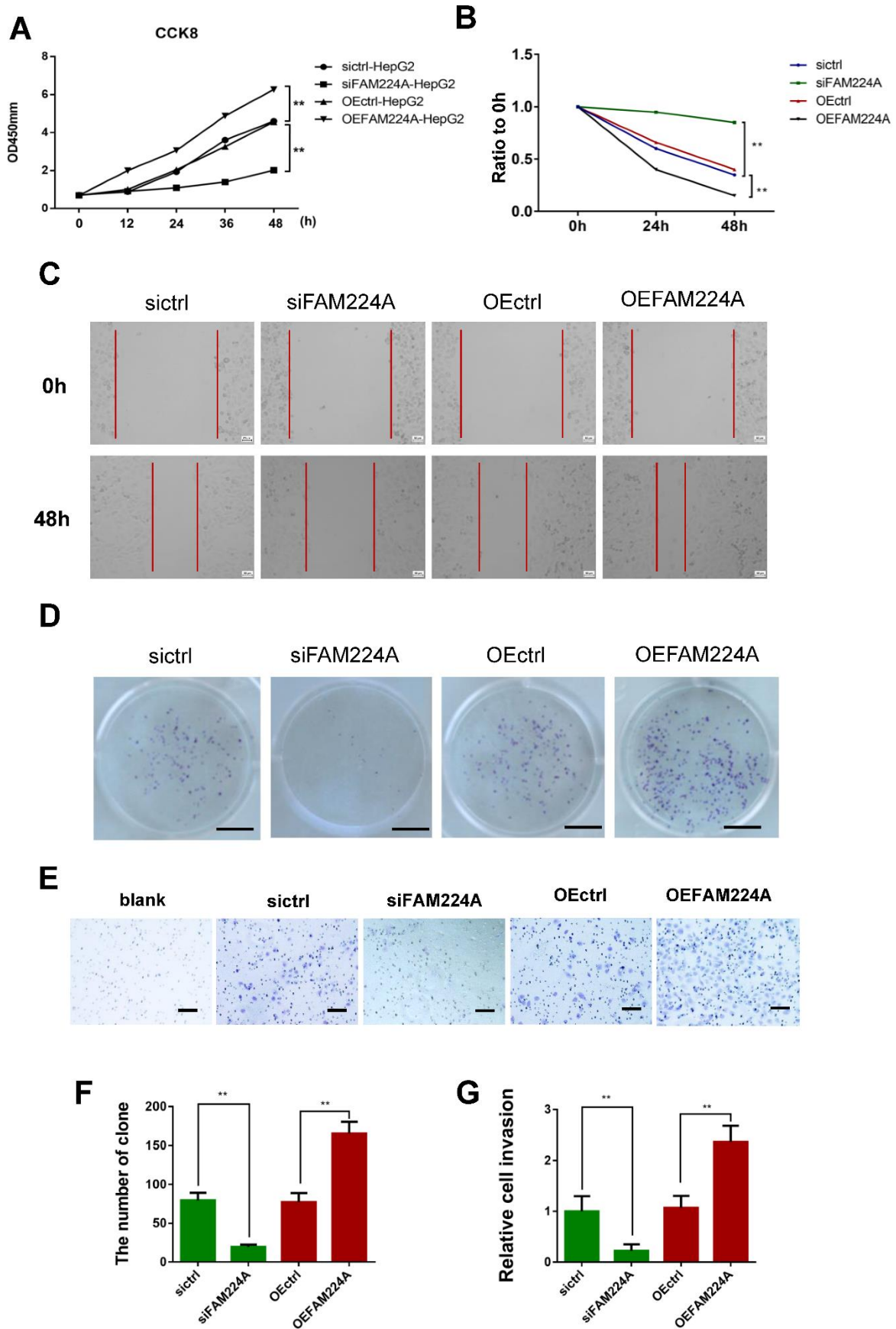


Figure 6. Effect of the changes in the FAM224A expression on multiple functions of HepG2 cells. (A) CCK-8 assay revealed that the multiplication ability of HepG2 cells improved as the FAM224A expression level increased. (B and C) Wound healing test, (D) cloning formation assays, and (E) Transwell assays on HepG2 cells were performed. (F) Statistical results of the cell clone numbers in Figure D were obtained. (G) Statistical results of the cell invasion numbers in Figure E were determined. Mean \pm SD; *P < 0.05; **P < 0.01, ***P < 0.001.

Inhibition of tumor xenograft growth via FAM224A knockdown and hsa-mir-139 overexpression

An in vivo study suggested that the tumors from the FAM224A (-), hsa-mir-139, and FAM224A (-) + hsa-mir-139 groups were less than those from the control group (Figure 7A and 7B).

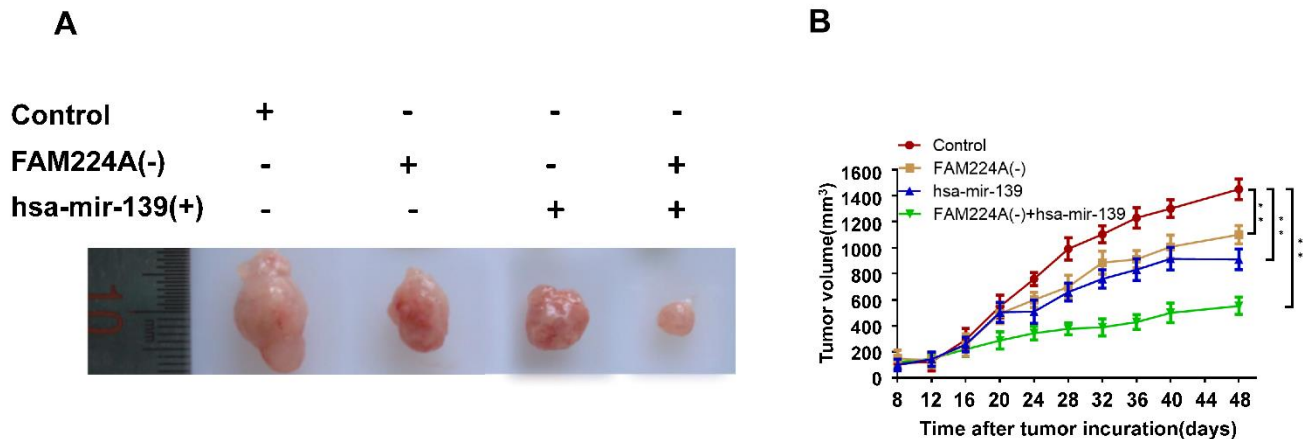


Figure 7. Knockdown of Inhibition of tumor xenograft growth via FAM224A knockdown and overexpression of hsa-mir-139 overexpression inhibited tumor xenograft growth. (A) Tumor samples from each group were provided. (B) The growth curves of tumor xenograft in subcutaneous implantation test were showed. Mean ± SD; *P < 0.05; **P < 0.01.

Table 3. qRT-PCR primers

RAD54B	Forward	5' - GCCAAACACTGATGATTTGTGG - 3'
	Reverse	5' - CCTGAGAAGAATGCGAGATAGC - 3'
FAM224A	Forward	5'-TCTCCACCTCCTTGCTTCC-3'
	Reverse	5'-TTTAAACAAGCCAGCCAAGC-3'
hsa-miR-139	Forward	5'-TCTACAGTGCACGTGTCTCCAG-3'
	Reverse	5'-ACGCAAATTCGTGAAGCGTT-3'
Beta-actin	Forward	5' - AGCACAGAGCCTCGCCTTTG - 3'
	Reverse	5' - CTTCTGACCCATGCCACCA - 3'
U6	Forward	5'-CTCGCTTCGGCAGCACA-3'
	Reverse	5'-AACGCTTCACGAATTTGCGT-3'

DISCUSSION

Over the years, the importance of lncRNAs has been widely acknowledged because of their biological functions and effects on tumor progression and metastasis [23-25]. lncRNAs constitute the main part of the ceRNA network and act as miRNA sponges to regulate genetic transcription, but the exact role of lncRNA-associated ceRNA in liver cancer is unclear.

Several studies have reported the function of lncRNAs and their related ceRNA network in hepatic carcinoma. Xie and coauthors [26] discovered an HCAL-miR-15a/miR-196a/miR-196b-LAPTM4B network and demonstrated that HCAL may be a target for hepatic carcinoma treatment. Li and coauthors [27] demonstrated that LINC00346-miR-10a-5p-CDK1 network plays an important role in HBV-related hepatic carcinoma. Wu and coauthors [28] showed that the KRAL/miR-141/Keap1 axis participates in the tolerance of hepatic carcinoma cells to 5-fluorouracil. Liu and coauthors [29] found that in probing the molecular mechanisms of hepatic carcinoma, lncRNA SNHG1 and SNHG3-related ceRNAs have enormous research potential. Lin and coauthors [30] performed a whole-genome analysis of prognostic lncRNAs, miRNAs, and mRNAs that form an endogenous RNA network in hepatic carcinoma. Yue and coauthors [31] distinguished possible prognostic genes and set up a hepatic carcinoma regulatory network in lncRNA-miRNA-mRNA ceRNA.

In the present study, liver cancer-associated DElncRNAs, DEmRNA, and DEMiRNA were identified in the expression profile sequencing data from TCGA database. 2,699 DElncRNAs, 320 DEMiRNAs, and 6,356 DEmRNAs were identified in liver cancer and paracarcinoma tissues, and a liver cancer-specific ceRNA

network was set up. The co-expression network of lncRNA–miRNA–mRNA was established on the basis of the relationships between mRNAs, lncRNAs, and miRNAs. Subsequently, molecules in ceRNA networks were screened and found to be novel prognostic factors and treatment targets of liver cancer. Then, 2 miRNAs, 10 lncRNAs, and 46 mRNAs were identified by the network. Finally, FAM224A/hsa-mir-139/RAD54B was identified as a potential ceRNA.

FAM224A is one antisense gene of the sequence similarity 224 member A gene and its expression levels indicate a poor prognosis of patients with glioma [32]. However, the function of the lncRNA family, specifically FAM224A, in liver cancer has not been reported. hsa-mir-139 has a vital function in hepatic carcinoma. It is located within the second intron of the phosphodiesterase 2A gene on chromosome 11q13.4 and often underexpressed in HCC. miR-139 mainly plays an inhibitory role in hepatic carcinoma; it can suppress the multiplication, migration, and invasion of hepatic carcinoma cells [33, 34]. Human RAD54B is an important DNA repair and recombination protein [35]. Moreover, the RAD54B expression level is increased in liver cancer tissues.

In our research, we found that FAM224A negatively regulated the hsa-mir-139 expression and positively regulated the RAD54B expression in liver cancer. Dual-luciferase assays verified that hsa-mir-139 could bind to FAM224A and RAD54B, which were both included in an RNA-induced silencing complex. Furthermore, FAM224A knockdown upregulated the hsa-mir-139 expression and decreased the RAD54B expression. hsa-mir-139 played an inhibitory role in hepatic carcinoma. It is negatively regulated by the spongiform action of miRNA of FAM224A. Additionally, RAD54B exerted an oncogenic role in hepatic carcinoma. hsa-mir-139 could bind to RAD54B 3'UTR and negatively regulate RAD54B, hindering the malignant progression of liver cancer. Furthermore, the expression level of RAD54B could be promoted via feedback by FAM224A, and FAM224A enhanced the multiplication, migration and invasion of hepatic carcinoma cells.

Only one type of cell line was involved in our experimental studies; as such, this condition could affect the reliability of our results. Thus, the mechanism in all cancer types should be further explored.

CONCLUSION

In conclusion, we identified a FAM224A/hsa-mir-139/RAD54B network in liver cancer and revealed that FAM224A might be an important prognostic factor and potential treatment target for liver cancer. Furthermore, we recommended comprehensive animal studies and clinical trials to verify our results.

Funding: This study was supported by the Chun Feng scientific research fund project of Tianjin First Central Hospital(2019CF17).

Conflicts of Interest: The authors declare no competing interests.

REFERENCES

- Petrick JL, Braunlin M, Laversanne M, Valery PC, Bray F, McGlynn KA. International trends in liver cancer incidence, overall and by histologic subtype, 1978-2007. *Int J Cancer*. 2016;139(7):1534-45.
- Villanueva A, Minguez B, Forner A, Reig M, Llovet JM. Hepatocellular carcinoma: novel molecular approaches for diagnosis, prognosis, and therapy. *Annu Rev Med*. 2010;61:317-28.
- Anwanwan D, Singh SK, Singh S, Saikam V, Singh R. Challenges in liver cancer and possible treatment approaches. *Biochim Biophys Acta Rev Cancer*. 2020;1873(1):188314.
- Chen B, Pan Y, Xu X, Wu F, Zheng X, Chen SY, et al. Inhibition of EPS8L3 suppresses liver cancer progression and enhances efficacy of sorafenib treatment. *Biomed Pharmacother*. 2020;128:110284.
- Cech TR, Steitz JA. The noncoding RNA revolution-trashing old rules to forge new ones. *Cell*. 2014;157(1):77-94.
- Liu Y, Liu X, Lin C, Jia X, Zhu H, Song J, et al. Noncoding RNAs regulate alternative splicing in Cancer. *J Exp Clin Cancer Res*. 2021;40(1):11.
- Matsui M, Corey DR. Non-coding RNAs as drug targets. *Nat Rev Drug Discov*. 2016;16(3):167.
- Network TCGA. Integrated genomic and molecular characterization of cervical cancer. *Nature*. 2017;543(7645):378-84.
- Mendell JT. Targeting a Long Noncoding RNA in Breast Cancer. *N Engl J Med*. 2016;374(23):2287-9.
- Tan D, Chong FT, Leong HS, Toh SY, Lau DP, Kwang XL, et al. Long noncoding RNA EGFR-AS1 mediates epidermal growth factor receptor addiction and modulates treatment response in squamous cell carcinoma. *Nat Med*. 2017;23(10):1167.
- Wang P, Xu J, Wang Y, Cao X. An interferon-independent lncRNA promotes viral replication by modulating cellular metabolism. *Science*. 2017;358(6366):págs. 1051-5.
- Miao Y, Ajami NE, Huang TS, Lin FM, Lou CH, Wang YT, et al. Enhancer-associated long non-coding RNA LEENE regulates endothelial nitric oxide synthase and endothelial function. *Nat Commun*. 2018;9(1):292.
- Wong CM, Tsang FH, Ng IO. Non-coding RNAs in hepatocellular carcinoma: molecular functions and pathological implications. *Nat Rev Gastroenterol Hepatol*. 2018;15(3):137.

14. Salmena L, Poliseno L, Tay Y, Kats L, Pandolfi PP. ceRNA hypothesis: The Rosetta Stone of a hidden RNA language? *Cell*. 2011;146(3):353-8.
15. Correia de Sousa M, Gjorgjieva M, Dolicka D, Sobolewski C, Foti M. Deciphering miRNAs' Action through miRNA Editing. *Int J Mol Sci*. 2019;20(24).
16. Stavast CJ, Erkeland SJ. The Non-Canonical Aspects of MicroRNAs: Many Roads to Gene Regulation. *Cells*. 2019;8(11).
17. Bossi L, Figueroabossi N. Competing endogenous RNAs: a target-centric view of small RNA regulation in bacteria. *Nat Rev Microbiol*. 2016;14(12).
18. Karreth F, Reschke M, Ruocco A, Ng C, Chapuy B, Léopold V, et al. The BRAF Pseudogene Functions as a Competitive Endogenous RNA and Induces Lymphoma InVivo. *Cell*. 2015;161(2):319-32.
19. Kumar MS, Armenterosmonterroso E, East P, Chakravorty P, Matthews N, Winslow MM, et al. HMGA2 functions as a competing endogenous RNA to promote lung cancer progression. *Nature*. 2014;505(7482):212-7.
20. Yang C, Wu D, Gao L, Liu X, Jin Y, Wang D, et al. Competing endogenous RNA networks in human cancer: hypothesis, validation, and perspectives. *Oncotarget*. 2016;7(12):13479-90.
21. Liao X, Wang X, Huang K, Han C, Deng J, Yu T, et al. Integrated analysis of competing endogenous RNA network revealing potential prognostic biomarkers of hepatocellular carcinoma. *J Cancer*. 2019;10(14):3267-83.
22. Langfelder P, Zhang B, Horvath S. Defining clusters from a hierarchical cluster tree: the Dynamic Tree Cut package for R. *Bioinformatics*. 2008;24(5):719-20.
23. Chen X, Zhou Z, Zhang Z, Zhao C, Li J, Jiang J, et al. Puerarin inhibits EMT induced by oxaliplatin via targeting carbonic anhydrase XII. *Front Pharmacol*. 2022;13:969422.
24. Jiang J, Li J, Zhou X, Zhao X, Huang B, Qin Y. Exosomes Regulate the Epithelial-Mesenchymal Transition in Cancer. *Front Oncol*. 2022;12:864980.
25. Eptaminitaki GC, Wolff N, Stellas D, Sifakis K, Baritaki S. Long Non-Coding RNAs (lncRNAs) in Response and Resistance to Cancer Immun-surveillance and Immunotherapy. *Cells*. 2021;10(12).
26. Xie CR, Wang F, Zhang S, Wang FQ, Zheng S, Li Z, et al. Long Noncoding RNA HCAL Facilitates the Growth and Metastasis of Hepatocellular Carcinoma by Acting as a ceRNA of LAPTM4B. *Mol Ther Nucleic Acids*. 2017;9(C):440-51.
27. Li H, Zhao X, Li C, Sheng C, Bai Z. Integrated analysis of lncRNA-associated ceRNA network reveals potential biomarkers for the prognosis of hepatitis B virus-related hepatocellular carcinoma. *Cancer Manag Res*. 2019;11:877-97.
28. Wu L, Pan C, Wei X, Shi Y, Zheng J, Lin X, et al. lncRNA KRAL reverses 5-fluorouracil resistance in hepatocellular carcinoma cells by acting as a ceRNA against miR-141. *Cell Commun Signal*. 2018;16(1):47.
29. Liu J, Li W, Zhang J, Ma Z, Wu X, Tang L. Identification of key genes and long non-coding RNA associated ceRNA networks in hepatocellular carcinoma. *PeerJ*. 2019;7:e8021.
30. Lin P, Wen DY, Li Q, He Y, Yang H, Chen G. Genome-Wide Analysis of Prognostic lncRNAs, miRNAs, and mRNAs Forming a Competing Endogenous RNA Network in Hepatocellular Carcinoma. *Cell Physiol Biochem*. 2018:1953-67.
31. Yue C, Ren Y, Ge H, Liang C, Xu Y, Li G, et al. Comprehensive analysis of potential prognostic genes for the construction of a competing endogenous RNA regulatory network in hepatocellular carcinoma. *Onco Targets Ther*. 2019;12:561-76.
32. Song Y, Shao L, Xue Y, Ruan X, Liu X, Yang C, et al. Inhibition of the aberrant A1CF-FAM224A-miR-590-3p-ZNF143 positive feedback loop attenuated malignant biological behaviors of glioma cells. *J Exp Clin Cancer Res*. 2019;38(1):248.
33. Zan Y, Wang B, Liang L, Deng Y, Tian T, Dai Z, et al. MicroRNA-139 inhibits hepatocellular carcinoma cell growth through down-regulating karyopherin alpha 2. *J Exp Clin Cancer Res*. 2019;38(1):182.
34. He H, Wang Y, Ye P, Yi D, Cheng Y, Tang H, et al. Long noncoding RNA ZFPM2-AS1 acts as a miRNA sponge and promotes cell invasion through regulation of miR-139/GDF10 in hepatocellular carcinoma. *J Exp Clin Cancer Res*. 2020;39(1):159.
35. Bohl SR, Schmalbrock LK, Bauhuf I, Meyer T, Dolnik A, Szyska M, et al. Comprehensive CRISPR-Cas9 screens identify genetic determinants of drug responsiveness in multiple myeloma. *Blood Adv*. 2021;5(9):2391-402.



© 2022 by the authors. Submitted for possible open access publication under the terms and conditions of the Creative Commons Attribution (CC BY NC) license (<https://creativecommons.org/licenses/by-nc/4.0/>).